EPJ Web of Conferences **118**, 01005 (2016) DOI: 10.1051/epjconf/201611801005
FCCP2015

The muon EDM in the g-2 experiment at Fermilab

Rebecca Chislett[1,a] *on behalf of the* Muon $g-2$ Collaboration[b]

[1] *Department of Physics and Astronomy, UCL, London, WC1E 6BT, UK.*

Abstract. The observation of a muon electric dipole moment would provide an additional source of CP violation which is required to explain the matter anti-matter asymmetry in the universe. The current experimental limit, $|d_\mu| < 1.9 \times 10^{-19} e{\cdot}$cm, was set by the BNL E821 experiment. This paper discusses how the new experiment at Fermilab, E989 [3], aims to decrease this by two orders of magnitude down to $10^{-21} e{\cdot}$cm.

1 Introduction

The new g-2 experiment at Fermilab is designed to measure the anomalous part of the muon magnetic dipole moment (MDM) to a precision of 140ppb, an improvement over the 540ppb measurement made at the previous BNL E821 experiment [1]. However, it is also possible to make a measurement or set a limit on a possible muon electric dipole moment (EDM). The new experiment hopes to improve on the E821 limit of $|d_\mu| < 1.9 \times 10^{-19} e{\cdot}$cm [2] by about two orders of magnitude.

Theoretically, fundamental particles can have an EDM directed along the spin and governed by an equation analogous to the experimentally observed MDM,

$$\vec{d} = \eta \frac{Qe}{2mc} \vec{s}. \tag{1}$$

The Hamiltonian, $\mathcal{H}$, for a spin one-half particle in an electric (E) and magnetic (B) field for a particle with a magnetic moment, μ, is

$$\mathcal{H} = -\vec{\mu} \cdot \vec{B} - \vec{d} \cdot \vec{E}. \tag{2}$$

Considering the transformation properties of the various components, as shown in Table 1, it can be seen that the EDM component, $\vec{d} \cdot \vec{E}$ is a CP odd quantity. The present experimental limits [9–11] are orders of magnitude above the Standard Model predictions, hence any observed EDM would provide an additional source of CP violation. Since the CP violation in the Standard Model is insufficient to explain the matter-antimatter asymmetry in the universe the search for a new source is important. At the current levels of experimental precision the limits on EDMs have started to cut in to the predictions from different beyond the standard model (BSM) theories [5].

The present limit on the electron EDM, $8.7 \times 10^{-29} e{\cdot}$cm [9], is about 9 orders of magnitude smaller than the muon EDM limit. Assuming a simple mass scaling, $d \propto m$, the electron limit would indicate that the muon EDM would be less than $\sim 10^{-27}$, far below what can be measured currently. However, some BSM models [12, 13] predict non-standard scalings which are quadratic or even cubic in mass. The muon also provides a unique opportunity to search for an EDM in the second generation of particles.

Table 1. The transformation properties of the electric and magnetic fields and dipole moments

	$\vec{E}$	$\vec{B}$	$\vec{\mu}$ or $\vec{d}$
P	-	+	+
C	-	-	-
T	+	-	-

2 Experimental setup

The Fermilab E989 g-2 experiment is based on the same experimental setup as was used in the E821 experiment with some significant improvements to increase the precision [4]. Polarised muons are injected into the storage ring and as they travel around the ring the anomalous magnetic moment, a_μ, causes the spin to precess around faster than the muon momentum. The parity violation inherent in weak decays means that the highest energy positrons are emitted parallel to the muon spin. This allows the spin direction to be tracked through the detection of the decay positrons, done using 24 calorimeter stations around the ring.

The difference between the spin and cyclotron frequencies is given by

$$\vec{\omega}_a = -\frac{Qe}{m_\mu} \left[a_\mu \vec{B} - \left(a - \frac{1}{\gamma^2 - 1} \right) \frac{\vec{\beta} \times \vec{E}}{c} \right] \tag{3}$$

for $\beta \cdot B = \beta \cdot E = 0$. The experiment is run at the "magic" momentum $p_{magic} = m/\sqrt{a_\mu} = 3.09$ GeV/c, such that the equation simplifies to

[a] e-mail: rebecca.chislett.10@ucl.ac.uk

[b] `muon-g-2.fnal.gov/collaboration.html`

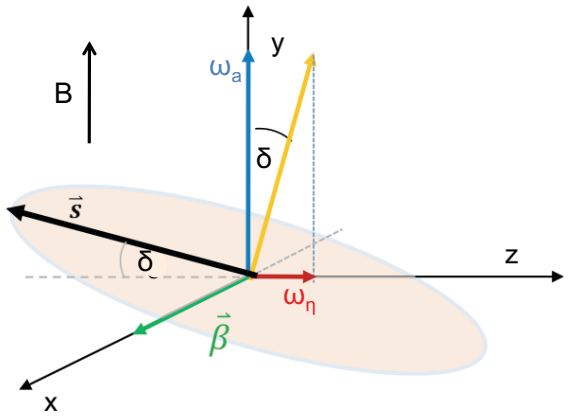

Figure 1. The contributions to the precession frequency from the MDM and the EDM and the resulting spin precession plane.

$$\vec{\omega}_a = -a_\mu \frac{Qe}{m_\mu}\vec{B}. \tag{4}$$

Therefore the anomalous magnetic moment can be determined using the precession frequency extracted from the positron decays and a precise measurement of the magnetic field. However, if the muon has an EDM the equation for the spin precession gains an extra component:

$$\vec{\omega}_\eta = -\eta\frac{Qe}{2m_\mu}\left[\frac{\vec{E}}{c} + \vec{\beta}\times\vec{B}\right]. \tag{5}$$

which add to $\vec{\omega}_a$.

The component of the spin precession from the MDM is directed along the magnetic field, causing the spin to precess in the horizontal plane. The contribution from the EDM is dominated by the motional magnetic field contribution, which is directed towards the centre of the ring, causing a vertical precession of the spin. Adding in the EDM component causes the spin precession plane to tilt, leading to a vertical oscillation $\pi/2$ out of phase with the precession due to the MDM. Assuming that the motional field dominates and the other components can be neglected, the two contributions are perpendicular as shown in Figure 1. The tilt in the precession plane is then given by

$$\delta = \tan^{-1}\left(\frac{\eta\beta}{2a}\right). \tag{6}$$

which produces a milliradian tilt for an EDM of the order of $10^{-19}e$·cm. The additional component from an EDM also slightly increases the magnitude of the precession frequency to:

$$\omega_{a\eta} = \sqrt{\omega_a^2 + \omega_\eta^2}. \tag{7}$$

This leads to two EDM search methods; indirectly, by comparing the measured value of the precession frequency to the Standard Model prediction or directly, by looking for a tilt in the precession plane. Three different direct analyses were performed at the E821 experiment to look for a vertical oscillation, each of which will be discussed in turn along with the possible improvements to the measurements at the new experiment.

3 Measuring the EDM at E821

The E821 EDM measurement was a combination of three different analyses. The first two used scintillator panels on the front of the calorimeter to divide the calorimeter into vertical (and horizontal in some cases) segments. One looked for an oscillation in the average vertical position of the positrons hitting the calorimeter [8] and the other looked for a asymmetry in the phases as a function of vertical position [7]. Both of these measurements were dominated by systematic uncertainties. The third measurement, dominated by statistical uncertainties, used the tracking detector to look for an oscillation in the positron decay angle as a function of time [6].

For a fixed magnetic field and muon momentum the statistical figure of merit is given by NA^2 where N is the total number of positrons and A is the asymmetry. In the case of the MDM this asymmetry is the difference between forward and backward going spins, whereas for the EDM it is the difference between upward and downward going spins. Figure 2 shows this figure of merit as a function of energy for both the MDM and EDM. In the case of the forward-backward asymmetry of the MDM this results in a greater statistical power for positrons at the higher end of the energy spectrum, whereas in the case of the EDM the acceptable energy range is much broader and centred further toward the middle of the energy spectrum. Hence in the EDM search considering a wider range of positron energies is preferable.

3.1 Vertical Position Oscillations

A tilt in the precession plane would cause an oscillation in the vertical angle of the positrons, leading to an oscillation in the average vertical position of the positrons hitting the calorimeter. However, changes in the path length of the positrons hitting the calorimeter cause the vertical width to vary which can feed in to oscillations in the average vertical position if the calorimeter isn't perfectly aligned. To quantify this effect the average width is plotted as a function of time. This distribution is then fit to obtain the different contributions:

$$\begin{aligned} f(t) =& W + S_{g2}sin(\omega t) + C_{g2}cose(\omega t) \\ &+ S_{2g2}sin(2\omega t) + C_{2g2}cos(2\omega t) \\ &+ e^{-t/\tau_{CBO}}\left[S_{CBO}sin\left(\omega_{CBO}(t-t_0)+\Phi_{CBO}\right)\right. \\ &\qquad \left. + C_{CBO}cos\left(\omega_{CBO}(t-t_0)+\Phi_{CBO}\right)\right] \\ &+ L(t) \end{aligned} \tag{8}$$

The first term is the average width. The second set of terms are oscillations in phase with the g-2 oscillation due to the difference in path length between positrons from different spin orientations. Those that travel further to reach the calorimeter will have a greater vertical spread

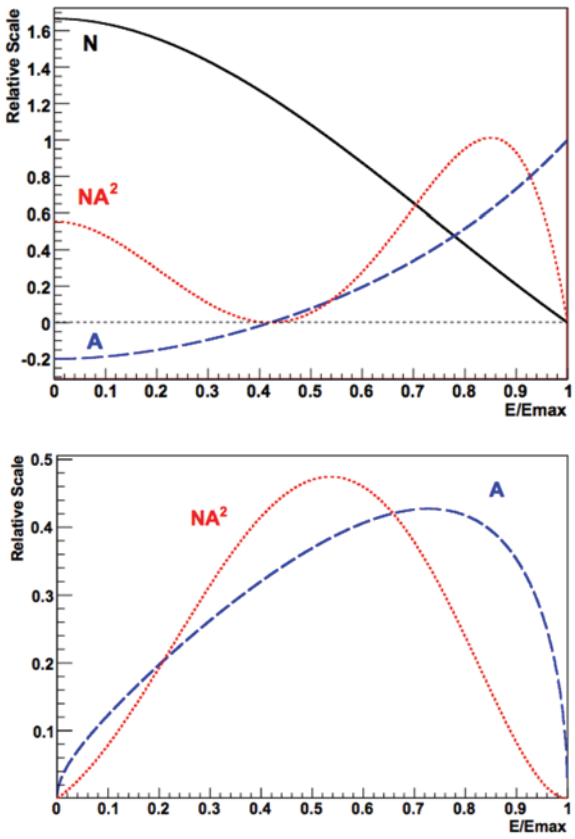

Figure 2. The statistical figures of merit for the MDM measurement (top) and EDM measurement (bottom) as a function of normalised positron energy [2].

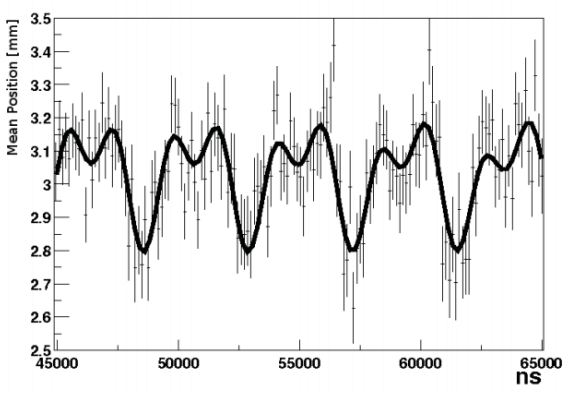

Figure 3. The average vertical position of the positrons hitting the calorimeter as a function of time [2].

Table 2. The uncertainties associated with the vertical position oscillation measurements [2].

Effect	Error(μm)
Detector Tilt	6.1
Vertical Spin	5.1
Quadrupole Tilt	3.9
Timing Offset	3.2
Energy Calibration	2.8
Radial Magnetic Field	2.5
Albedo and Doubles	2.0
Fitting Method	1.0
Total Systematic	10.4
Statistical	5.9
Total Uncertainty	11.9

by the time they reach the calorimeter, despite being released with the same variation in decay angles. The g-2 frequency is fixed in the fit using the number oscillation results. Lastly, coherent betatron oscillations (CBO) cause variations in the radial position of the beam and hence the distance the positrons travel, again changing the width on the face of the calorimeter. The final term accounts for the calorimeter deadtime which has a greater impact at earlier times.

The CBO frequency, phase and lifetime extracted from the width oscillations are then fixed in the fit to the average vertical position as a function of time, shown in Figure 3. The fit function used is similar to that for the width oscillations,

$$\begin{aligned} f(t) =& K + \left[S_{g2}sin(\omega t) + C_{g2}cos(\omega t)\right] \\ &+ e^{-t/\tau_{CBO}}\left[S_{CBO}sin\left(\omega_{CBO}(t-t_0)+\Phi_{CBO}\right)\right. \\ &\qquad \left. + C_{CBO}cos\left(\omega_{CBO}(t-t_0)+\Phi_{CBO}\right)\right] \\ &+ Me^{-t/\tau_M} \end{aligned} \tag{9}$$

where the first term is the average vertical position, the second accounts for variations at the g-2 frequency, the third corresponds to CBO oscillations and the final term is for slow changes in detector response and pileup. As the g-2 number oscillation is aligned with the cosine phase an EDM signal would show up as a non zero value of S_{g2}.

The systematic uncertainties associated with this measurement are summarised in Table 2. The largest systematic comes from the calorimeter potentially being tilted with respect to the beam, such that any horizontal oscillation also appears as a vertical oscillation. An average vertical muon spin component pushes the decay angles off centre and when combined with the varying positron path lengths causes a vertical oscillation. Any radial magnetic field would also have a similar effect due to the deflection of the positrons. It is also important to consider any difference between the top and bottom halves of the calorimeter which could fake an oscillation. Overall, the systematic uncertainties are much larger than the statistical uncertainties and so it is a priority of the E989 experiment to reduce these, as will be detailed in Section 4.

The final measurement of the average vertical position oscillations is $S_{g2} = (1.27 \pm 11.9)\mu$m, which based on simulation translates to an EDM measurement of $d_\mu = (-0.1 \pm 1.4) \times 10^{-19} e$·cm. The resulting limit with 95% confidence level sets the limit as $|d_\mu| < 2.8 \times 10^{-19} e$·cm.

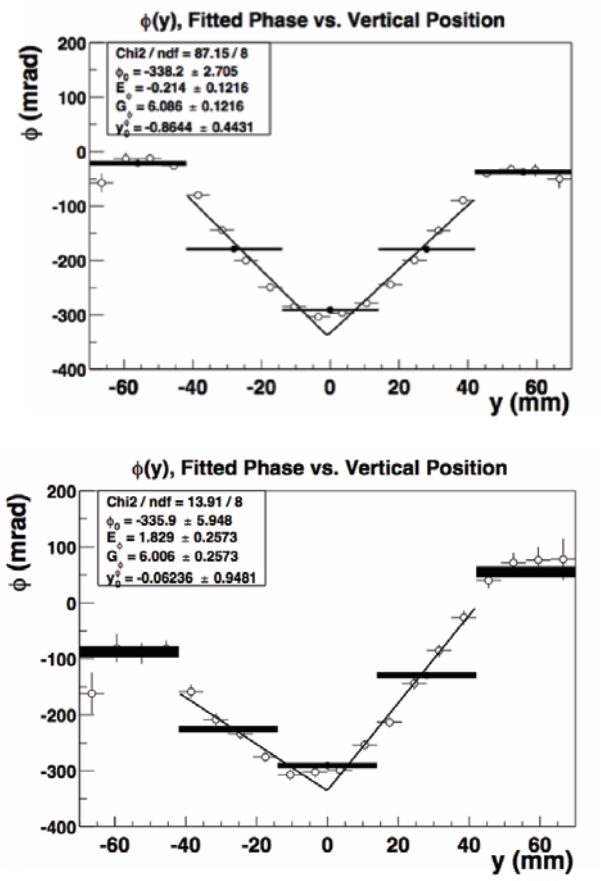

Figure 4. The fitted phase as a function of the vertical position from simulation with no EDM (top) and with an EDM (bottom) [7].

3.2 Vertical phase asymmetry

The positrons emitted in the outward radial direction have a longer path length to the detector and therefore have a larger vertical spread on the calorimeter face. This means that the positrons detected towards the top and bottom are dominated by outward going decays and those in the centre by the inward going positrons leading to a change in the fitted phase with the vertical position. However, the presence of an EDM would tilt the precession plane and lead to more outward going decays in the top half of the calorimeter and more inward going decays at the bottom, suppressing the phase difference in the bottom half of the calorimeter and leading to an asymmetry in the distribution. This effect is shown using simulated events in Figure 4.

The phase as a function of vertical position can be fitted to look for an EDM contribution:

$$\Phi(y) = p_0 + p_1(y - p_2) + |p_3(y - p_2)|. \quad (10)$$

The first term is the value at the centre of the calorimeter, and the last is the symmetric phase shift expected without the presence of an EDM. A non-zero value of the parameter p_1 would be the indication of an asymmetry in the phase and hence of an EDM.

Table 3. The uncertainties associated with the vertical phase asymmetry measurements [2].

Effect	Error(μrad / mm)
Detector Tilt	20
Detector Misalignment	28
Energy Calibration	4.3
Muon Vertical Spin	8.0
Radial Magnetic Field	14.4
Timing	3.4
Total Systematic	38
Statistical	28
Total Uncertainty	47

The systematic uncertainties on this measurement, as shown in Table 3, are similar to those for the vertical position measurement. The dominant uncertainties come from a misalignment or tilt in the calorimeters, where a misalignment can fake an asymmetry by shifting the spectrum slightly off centre and a tilt can cause asymmetric vertical loses again inducing a fake signal. Any non zero average vertical spin or radial magnetic field also has an effect for similar reasons to the discussion in Section 3.1

3.3 Vertical decay angle

The final method used to search for an EDM signal used the tracking detector placed in front of one of the calorimeter stations. This allows for a more direct measurement of the angle of the decaying positrons, but is more statistically limited than the other measurements. Firstly the number oscillation was plotted as a function of time. This was done modulo the precession period to reduce the effects of periodic disturbances at other frequencies. Fitting the distribution provides the phase of the g-2 oscillation:

$$N(t) = e^{-t/\tau_e}(N_0 + Wcos(\omega t + \Phi)). \quad (11)$$

This phase can then be used in the fit to the vertical angle oscillation:

$$\theta(t) = M + A_\mu cos(\omega t + \Phi) + A_{EDM} sin(\omega t + \Phi). \quad (12)$$

as shown in Figure 5. The first term accounts for any offset in the central angle, which could be due to an average vertical muon spin component. The second term is in phase with the number oscillation and the final term is out of phase, where a non zero value of A_{EDM} indicates the presence of an EDM.

The systematic uncertainties associated with this measurement are small compared to the statistical uncertainty, as shown in Table 4. The largest contributions are from any coupling of the CBO oscillations into the vertical decay angle and the acceptance coupling. The acceptance coupling refers to the variation of vertical angle acceptance of the detector with azimuth combined with the correlation between the positron path length and azimuthal position of the decay point. Other contributions that were considered include a radial magnetic field, which would

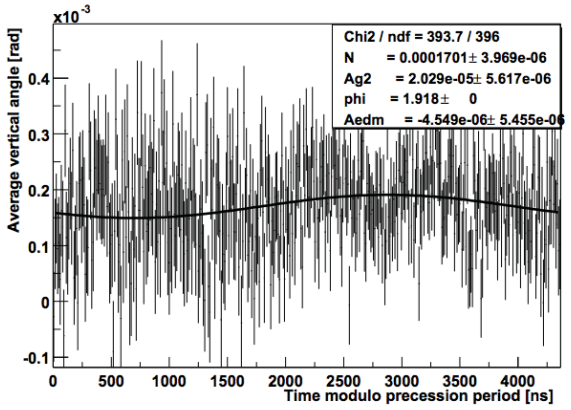

Figure 5. The average vertical decay angle as a function of time modulo the precession period [2].

Table 4. The uncertainties associated with the vertical decay angle measurement [2].

Effect	Error(μrad)
Radial Magnetic Field	0.13
Acceptance Coupling	0.3
Horizontal CBO	0.3
Phase Fit	0.01
Precession Period	0.01
Total Systematic	0.44
Statistical	4.4
Total Uncertainty	4.4

tilt the precession plane, and errors due to the fit. Most of the systematic error estimates are very conservative but despite this remain an order of magnitude below the statistical uncertainties.

In this analysis the measured vertical angle oscillation amplitude was $(-0.1 \pm 4.4) \times 10^{-6}$ rad which produces a limit of $|d_\mu| < 3.2 \times 10^{-19} e$·cm.

4 Improvements at E989

The new g-2 experiment at Fermilab has many upgrades which will increase the sensitivity to an EDM signal. The easiest measurement to improve upon is the vertical decay angle measurement as the number of positron decays recorded by the trackers will be increased at the new experiment. However, it is worth discussing the changes that might reduce the systematic uncertainties on the calorimeter-based analyses.

Firstly, the calorimeters at E989 will be segmented, using a grid of 6 by 9 cells, removing the need for scintillators to be placed on the front to make the measurements. This segmentation will help with the ability to control pileup and measure both the detector position and detector tilt, both large sources of systematic uncertainty in the E821 EDM measurement. The lower energy acceptance of the new calorimeters is important for EDM measurements as the sensitivity covers a broader energy range than the g-2 number oscillation measurement. In addition a laser calibration system is being introduced to improve the gain calibration and timing information.

Secondly, the electrostatic quadrupole voltage at E989 has been chosen carefully to reduce the amplitude of the CBO by at least a factor of 4. This will impact all three analyses as the CBO was a significant systematic uncertainty. The new E989 experiment will have three straw tracking detectors, compared to the one present at E821 which, although not directly used in the calorimeter analyses, improves the knowledge and monitoring of the beam distribution. The full BMAD and G4Beamline simulations all the way from the production target will provide detailed information on the polarisation and momentum variance of the beam. Lastly, the increased amount of data will not only reduces the statistical uncertainty, but will also decrease the systematic uncertainties that are derived from the data.

All of the improvements mentioned above help to reduce the systematic uncertainties on the calorimeter-based EDM measurement, although the total reduction is yet to be quantified. However, the most promising measurement for the E989 experiment is the vertical decay angle, which will be vastly improved by the increase in the number of muons, the number of trackers and the increased tracker acceptance. Combining these three effects the new experiment is expected to take of the order of 1000 times more statistics than at E821, which should reduce the statistical error by one order of magnitude quickly and further subsequently.

Obviously, once the statistical error is reduced by an order of magnitude the systematic uncertainties start to become important and need to be controlled. Most of the improvements mentioned above also apply to this measurement, most importantly the reduction in the CBO. The fact that the tracker is placed inside the vacuum chamber and has an increased geometrical acceptance makes a significant difference, especially for the acceptance-coupling uncertainty. The trackers will also provide a much improved characterisation of the beam and the alignment of the calorimeters which are critical to achieving the goal of an EDM sensitivity down to $10^{-21} e$·cm.

5 Conclusions

The new g-2 experiment aims to improve the limit on the muon EDM set at the previous E821 experiment at BNL by approximately two orders of magnitude, down to 10^{-21}e·cm. Three different methods, each with a similar sensitivity, were combined to set the previous limit and the improvements to the new experiment mean that a lower limit will be reached in all of these analyses. However, with the introduction of three new tracking stations, the most promising method searches for an oscillation in the average vertical decay angle of the positrons, which was statistics limited at E821 with low systematic errors. At the new experiment the tracking statistics are expected to increase by about 1000 times, and this coupled with an improved understanding of the key systematic uncertainties will allow and EDM of 10^{-21}e·cm to be probed.

Acknowledgments

The Fermilab $g-2$ experiment is supported in part by the U.S. DOE Offices of High-Energy and Nuclear Physics, the U.S. NSF, the U.K. STFC, the NSFC in China, the XXX in Korea, and by the INFN in Italy. The author is supported by the DOE Office of Nuclear Physics, award DE-FG02-97ER41020.

This work was supported by the STFC grant: ST/L001888/1.

References

[1] E821 Collaboration, G. W. Bennett, et al., Phys. Rev. Lett **92**, 161802 (2004).

[2] E821 Collaboration, G. W. Bennett, et al., Phys. Rev. D **80**, 052008 (2009).

[3] E989 Collaboration, J. Grange et al., FERMILAB-FN-0992-E (2015).

[4] D. Hertzog, this workshop, *Next Generation Muon g-2 Experiments* (2015).

[5] J. Engle, et al., Prog. Part. Nucl. Phys. **71** (2013) 21-74

[6] M. Sossong, *A Search for an Electric Dipole Moment of the Positive Muon)*, University of Illinois PhD thesis(2005).

[7] S. O. Giron, *Measuring the Electric-Dipole Moment of the Muon at BNL E821*, University of Minnesota PhD thesis(2004).

[8] R. S. McNabb, *An Improved Limit on the Electric Dipole Moment of the Muon*, University of Minnesota PhD thesis (2003).

[9] ACME Collaboration, J. Baron, et al., Science **343**, 269 (2014)

[10] W.C. Griffith, et al., Phys. Rev. Lett. **102**, 101601 (2009).

[11] C.A. Baker, et al., Phys. Rev. Lett. **97**, 131801 (2006).

[12] K.S. Babu, Bhaskar Dutta, R.N. Mohapatra, Phys. Rev. Lett. **85** 5064-5067 (2000).

[13] E. O. Iltan, Eur. Phys. J. C **54**, 583 (2008).